acquisition time (30 s). Concentration of each compound with respect to time was calculated by dividing the integral of resonance by the integral of fluorene internal standard. The concentrations were then plotted versus time to give the reaction profiles. The natural logarithm (ln) of the concentration of the complex could then be plotted versus time, which provided the first-order rate constants (k_1 = −(slope)) from linear least-squares analysis. Activation parameters were determined by plotting ln (k/T) versus $1/T$ (K^{-1}) at 60, 70, and 80 °C, where $\Delta H^{\ddagger} = -R$(slope) in cal/mol and $\Delta S^{\ddagger} = R$(y intercept −ln (k/h)) in eu (R = ideal gas constant, k = Boltzmann constant; h = Planck constant).

NMR Observation and Kinetics of the Thermal Decomposition of 13b. Decomposition of **13b** was observed and the kinetics were studied at 90, 100, and 110 °C in the same way as above. The reaction was followed by monitoring the methoxyl proton resonances of **13b** and the ester product and the methylene proton resonance (CH_2) of the fluorene internal standard. The reaction rates and activation parameters ($\Delta H^{\ddagger}$ and $\Delta S^{\ddagger}$) are reported in Table IV.

NMR Observation and Kinetics of the Thermal Decomposition of 13c. Since complex **13c** is not soluble in toluene, the decomposition was carried out in C_6D_5Cl (0.450 mL) at 60, 70, and 80 °C. Otherwise, the experiment was accomplished in the same way as above. The reaction was followed by monitoring the methoxyl proton resonances of **13c** and the ester product, and the methylene resonance (CH_2) of the fluorene internal standard. The reaction rates and activation parameters ($\Delta H^{\ddagger}$ and $\Delta S^{\ddagger}$) are listed in Table IV.

NMR Observation of Phosphine Inhibition on the Thermal Decomposition of 13a. Triphenylphosphine samples (1.2, 2.1, 3.3, and 4.3 mg) were placed in thin-wall 5-mm NMR tubes; each was then charged with 0.450 mL of the stock solution of **13a** (0.035 M) in C_6D_5Cl. The reactions were accomplished at 80 °C in the same way as without adding Ph_3P. The natural logarithm (ln) of the concentration of **13a** was then plotted versus time. Induction periods ($T_{induction}$) were derived by extrapolating the curve to the initial concentration of **13a** (Figure 3), and then plotted versus the ratio of the phosphine concentration and the initial concentration of **13a** (Figure 4).

Acknowledgment. We are grateful to the NSF for financial support (Grant CHE 9101767) and to Johnson-Matthey, Inc., for the generous loan of K_2PtCl_4.

Registry No. **8a**, 119818-78-9; **8b**, 126876-16-2; **10**, 138855-99-9; **12a**, 125540-80-9; **12b**, 126876-18-4; **13a**, 126876-19-5; **13b**, 126876-20-8; **13c**, 138856-00-5.

Supplementary Material Available: Tables of crystal data, bond distances and angles, torsion angles, least-squares planes, positional parameters and thermal parameters (11 pages); a listing of structure factors (17 pages). Ordering information is given on any current masthead page.

Effect of Ring Size on NMR Parameters: Cyclic Bisphosphine Complexes of Molybdenum, Tungsten, and Platinum. Bond Angle Dependence of Metal Shieldings, Metal–Phosphorus Coupling Constants, and the ^{31}P Chemical Shift Anisotropy in the Solid State

Ekkehard Lindner,* Riad Fawzi, Hermann August Mayer, Klaus Eichele, and Wolfgang Hiller

Institut für Anorganische Chemie der Universität, Auf der Morgenstelle 18, W-7400 Tübingen 1, Germany

Received May 8, 1991

The ^{31}P chemical shift tensors of bis(phosphine) complexes of the type $[M][Ph_2P(CH_2)_nPPh_2]$ ([M] = $(OC)_4Mo$, $(OC)_4W$, Cl_2Pt; n = 1–5) and of *fac*-$(OC)_3Mo[PPh(CH_2CH_2PPh_2)_2]$ were determined by solid-state NMR techniques and correlated with structural features of the compounds. $\delta(^{31}P)$, $^1J_{M-P}$, and $\delta(M)$ show a dependence on the ring size in the solution NMR spectra of the four- to six-membered chelates; for larger rings this dependence vanishes. A model for the orientation of the ^{31}P shift tensor principal components within the molecular frame is proposed. Each tensor component displays a different dependence on the ring size; the isotropic shift is dominated by the component perpendicular to the ring plane. Changes in this component are explained in terms of variations of the M–P–C angles. Generally speaking, the behavior of each of the tensor components must be regarded as a complex interplay of all six bond angles at phosphorus. The crystal structure of $(OC)_4W[Ph_2P(CH_2)_4PPh_2]$ (**2d**) was determined by X-ray diffraction. Crystals of **2d** are monoclinic, space group $P2_1/n$, a = 1202.8 (1) pm, b = 1531.8 (1) pm, c = 1654.1 (2) pm, β = 104.72 (1)°, and Z = 4.

Introduction

Solution-state ^{31}P NMR spectroscopy has proved to be an invaluable experimental technique for understanding the chemistry and structure of phosphorus-containing molecules.[1] Important parameters in these studies are the chemical shift $\delta(^{31}P)$, the coupling constant J_{P-X} to an isotope active in NMR spectroscopy, or relaxation rate data. Since the chemical shift of heavier nuclei is such a small and sensitive effect, it has only been recently with larger and faster computing facilities that reasonably accurate theoretical calculations have been forthcoming,[2]

(1) (a) *Phosphorus-31 NMR Spectroscopy in Stereochemical Analysis: Organic Compounds and Metal Complexes*; Verkade, J. G., Quin, L. D., Eds.; VCH Publishers: Deerfield Beach, FL, 1987. (b) Pregosin, P. S.; Kunz, R. W. In *NMR Basic Principles and Progress*; Diehl, P., Fluck, E., Kosfeld, R., Eds.; Springer Verlag: Berlin, Heidelberg, New York, 1979; Vol. 16. (c) Gorenstein, D. G. In *Progress in NMR Spectroscopy*; Emsley, J. W., Feeney, J., Sutcliffe, L. H., Eds.; Pergamon Press: Oxford, U.K., 1983; Vol. 16, p 1.

(2) (a) Chesnut, D. B.; Foley, C. K. *J. Chem. Phys.* **1986**, *84*, 852. (b) Chesnut, D. B.; Foley, C. K. *Ibid.* **1986**, *85*, 2814. (c) Farrar, T. C.; Trudeau, J. D. *J. Phys. Chem.* **1990**, *94*, 6277. (d) Fleischer, U.; Schindler, M.; Kutzelnigg, W. *J. Chem. Phys.* **1987**, *86*, 6337. (e) Kutzelnigg, W.; Fleischer, U.; Schindler, M. In *NMR Basic Principles and Progress*; Diehl, P., Fluck, E., Kosfeld, R., Eds; Springer Verlag: Heidelberg, 1990; Vol. 23, p 165. (f) Bouman, T. D.; Hansen, A. E. *Chem. Phys. Lett.* **1990**, *175*, 292. (g) Wolinski, K.; Hinton, J. F.; Pulay, P. *J. Am. Chem. Soc.* **1990**, *112*, 8251.

0276-7333/92/2311-1033$03.00/0

though they are restricted to small, metal-free systems. Similarly, the factors determining spin–spin coupling constants not involving protons are not well understood, because of the possibility of several coupling mechanisms.[3]

Because of these problems, a correlation of spectral information to structural details is generally difficult. Within a series of mutually related compounds, the problems are often reduced to one structural parameter as the major contributor which determines the spectrum. In this way, several important and helpful rules were established.[4,5] One of them is the ring contribution Δ_R for phosphorus nuclei involved in chelate rings.[6] This effect has been well-known since one of the first publications about ^{31}P NMR studies on organometallic compounds.[7] It describes the definite dependence of $\delta(^{31}P)$ on the ring size.[6] Thus, compared to similar acyclic compounds, the signal of phosphorus in five-membered metallacycles is shifted 20–50 ppm to lower field, whereas the phosphorus resonances of four- and six-membered chelates are shifted 12–80 and 2–17 ppm toward higher field, respectively. Despite numerous studies considering this ring effect, no reasonable explanation exists, but deformations of bond angles were excluded in the case of the five-membered chelate complexes.[8]

The influence of molecular geometry on the ^{31}P chemical shift has long been recognized.[9] However, in most of the studies reported to date only solution data have been taken into account. The interacting Hamiltonian in a liquid sample is represented by isotropic chemical shift and scalar spin–spin interactions. All possible anisotropic interactions, namely chemical shift anisotropy and dipolar and scalar spin–spin interactions are averaged due to rapid isotropic molecular motion. Thus important information is lost, which is retained in the solid state and may be used to monitor the symmetry properties and the electronic state of the solid.[10]

In a previous paper[11] we investigated various series of acyclic and five- and six-membered chelate complexes of monotertiary phosphines with manganese, molybdenum, and tungsten by ^{31}P solid-state NMR spectroscopy. We determined the three principal components of the chemical shift tensor and demonstrated that the individual tensor components reacted with much greater sensitivity to the electronic environment of these complexes than the isotropic chemical shift. For example, changes of the ring size from six- to five-membered cycles are expressed by a single tensor component as a 150–180 ppm downfield shift.[11]

To elucidate the above mentioned ring contribution to the chemical shift, we expanded our investigations to four- to eight-membered ring systems, the bis(phosphine) complexes of $Ph_2P(CH_2)_nPPh_2$ (n = 1–5) with molybdenum, tungsten, and platinum. These are compounds often used in mechanistic[12] and various spectroscopic[13] studies as model compounds possessing different ring sizes. We wish to discuss the metal shift, the chemical shift anisotropy of phosphorus, and the interaction between ^{31}P and ^{195}Pt as dipolar and scalar coupling in the solid state in terms of the ring size and to correlate them with structural features of these complexes. A model is proposed for the orientation of the chemical shift tensor of phosphorus within the molecular frame in such phosphine–metal complexes.

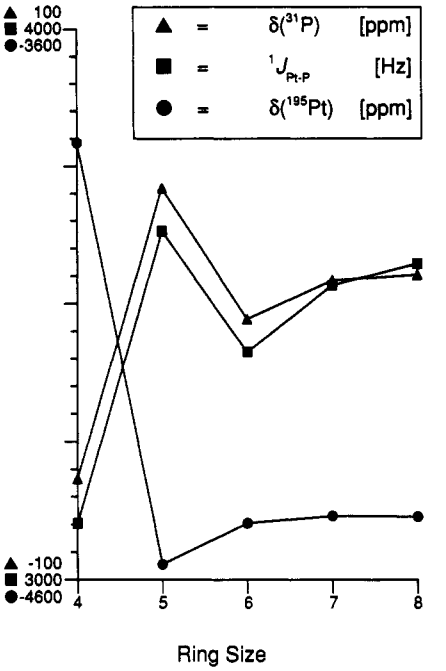

Figure 1. Dependence of $\delta(^{31}P)$ (▲), $^1J_{Pt-P}$ (■), and $\delta(^{195}Pt)$ (●) on the ring size in the solution NMR spectra of compounds $Cl_2Pt[Ph_2P(CH_2)_nPPh_2]$ [**3**, n = 1 (**a**), 2 (**b**), 3 (**c**), 4 (**d**), 5 (**e**)].

Chart I

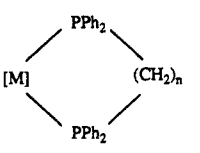

1-3

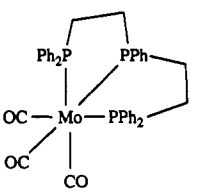

4

[M] = $Mo(CO)_4$ (1)
[M] = $W(CO)_4$ (2)
[M] = Cl_2Pt (3)

n	1	2	3	4	5
	a	b	c	d	e

Results and Discussion

The $^{31}P\{^1H\}$ NMR spectra of compounds **1–3** in solution exhibit one signal for two equivalent ^{31}P nuclei within the

(3) Finer, E. G.; Harris, R. K. In *Progress in Nuclear Magnetic Resonance Spectroscopy*; Emsley, J. W., Feeney, J., Sutcliffe, L. H., Eds.; Pergamon Press: Oxford, U.K., 1970; Vol. 6, p 61.
(4) Mann, B. E.; Master, C.; Shaw, B. L.; Slade, R. M.; Stainbank, R. E. *Inorg. Nucl. Chem. Lett.* **1971**, *7*, 881.
(5) Tolman, C. A. *Chem. Rev.* **1977**, *77*, 313.
(6) Garrou, P. E. *Chem. Rev.* **1981**, *81*, 229.
(7) Meriwether, L. S.; Leto, J. R. *J. Am. Chem. Soc.* **1961**, *83*, 3192.
(8) (a) Rehder, D.; Bechthold, H.-C.; Keçeci, A.; Schmidt, H.; Siewing, M. *Z. Naturforsch.* **1982**, *37B*, 631. (b) Hietkamp, S.; Stufkens, D. J.; Vrieze, K. *J. Organomet. Chem.* **1979**, *169*, 107. (c) Grim, S. O.; Del Gaudio, J.; Molenda, R. P.; Tolman, C. A.; Jesson, J. P. *J. Am. Chem. Soc.* **1974**, *96*, 3416. (d) Grim, S. O.; Briggs, W. L.; Barth, R. C.; Tolman, C. A.; Jesson, J. P. *Inorg. Chem.* **1974**, *13*, 1095. (e) Rehder, D. *J. Magn. Reson.* **1980**, *38*, 419. (f) Andrews, G. T.; Colquhoun, I. J.; McFarlane, W.; Grim, S. O. *J. Chem. Soc., Dalton Trans.* **1982**, 2353. (g) Lindner, E.; Fawzi, R.; Mayer, H. A.; Eichele, K.; Pohmer, K. *J. Organomet. Chem.* **1990**, *386*, 63. (h) Lindner, E.; Fawzi, R. *Ibid.* **1986**, *299*, C47.
(9) (a) Gutowsky, H. S.; McCall, D. W.; Slichter, C. P. *J. Chem. Phys.* **1953**, *21*, 279. (b) Callis, C. F.; Van Wazer, J. R.; Shoolery, J. N.; Anderson, W. A. *J. Am. Chem. Soc.* **1957**, *79*, 2719.
(10) Mehring, M. In *NMR Basic Principles and Progress*; Diehl, P., Fluck, E., Kosfeld, R., Eds.; Springer Verlag: Berlin, 1976; Vol. 11, p 1.
(11) Lindner, E.; Fawzi, R.; Mayer, H. A.; Eichele, K.; Pohmer, K. *Inorg. Chem.* **1991**, *30*, 1102.
(12) (a) Mukerjee, S. L.; Nolan, S. P.; Hoff, C. D.; de la Vega, R. L. *Inorg. Chem.* **1988**, *27*, 81. (b) Al-Salem, N. A.; Empsall, H. D.; Markham, R.; Shaw, B. L.; Weeks, B. *J. Chem. Soc., Dalton Trans.* **1979**, 1973. (c) Connor, J. A.; Day, J. P.; Jones, E. M.; McEwen, G. K. *Ibid.* **1973**, 347.
(13) (a) Gäbelein, H.; Ellermann, J. *J. Organomet. Chem.* **1978**, *156*, 389. (b) Bancroft, G. M.; Dignard-Bailey, L.; Puddephatt, R. J. *Inorg. Chem.* **1986**, *25*, 3675.

Table I. Chemical Shifts δ (ppm) and Coupling Constants *J* (Hz) of Compounds 1–4[a] in the ^{31}P, ^{195}Pt, ^{95}Mo, and ^{183}W Solution NMR and ^{31}P Solid-State NMR Spectra

compd	no.	δ(soln)[b]	$^1J_{M-P}$(soln)	δ_{iso}(solid)[c]	$^1J_{M-P}$(solid)	δ_{iso}(solid) − δ(soln)	δ(M)
$(OC)_4Mo$(dppm)	**1a**	0.1	110–122[d-f]	2.1	124	2.0	−1552[d,e]
				−3.6	124	−3.7	304[f]
$(OC)_4Mo$(dppe)	**1b**	53.8	128–145[d-g]	57.6	117	3.8	−1781[d,e,g]
				53.3	112	−0.5	80[f]
$(OC)_4Mo$(dppp)	**1c**	19.8	127–142[d-f]	13.7	95	−6.1	−1693[d,e]
							167[f]
$(OC)_4Mo$(dppb)	**1d**	27.9	133[d]	32.1		4.2	−1667[d]
				30.8		2.9	
				21.3		−6.6	
				20.4		−7.5	
$(OC)_4Mo$(dpppe)	**1e**	24.1		31.9		7.8	
				28.5		4.4	
				26.5		2.4	
				24.8		0.7	
				22.3		−1.8	
$(OC)_4W$(dppm)	**2a**	−25.6	201.2	−21.9	214	3.7	527[h]
				−27.0	210	−1.4	
$(OC)_4W$(dppe)	**2b**	38.6	228.5	42.7	197	4.1	192[h]
				37.5	213	−1.1	
$(OC)_4W$(dppp)	**2c**	−1.3	219.5	−6.4		−5.1	326[h]
$(OC)_4W$(dppb)	**2d**	9.5	228.5	16.7	181	7.2	367[h]
				7.0	184	−2.5	
$(OC)_4W$(dpppe)[i]	**2e**	7.1	228.1	16.8		9.7	
				10.5		3.4	
				4.8		−2.6	
Cl_2Pt(dppm)	**3a**	−63.5	3102	−65.9	3064	−2.4	−3808[k]
Cl_2Pt(dppe)	**3b**	41.9	3631	44.1	3591	2.2	−4572[k]
				36.7	3675	−5.2	
Cl_2Pt(dppp)	**3c**	−5.6	3412	−6.2	3354	−0.9	−4498[k]
Cl_2Pt(dppb)	**3d**	8.4	3533	26.4	3701	18.0	−4485[k]
				−6.4	3289	−14.8	
Cl_2Pt(dpppe)	**3e**	10.4	3572	26.5	3671	16.1	−4486[k]
				−6.4	3292	−16.8	
fac-$(OC)_3Mo$(etp)	**4**	81.3[l]	129–138[d,f,g]	84.8	112	3.5	−1760[d,g]
		53.9[m]		60.4	102	6.5	101[f]
				51.8	94	−2.1	

[a] Abbreviations: dppm = bis(diphenylphosphino)methane, dppe = 1,2-bis(diphenylphosphino)ethane, dppp = 1,3-bis(diphenylphosphino)propane, dppb = 1,4-bis(diphenylphosphino)butane, dpppe = 1,5-bis(diphenylphosphino)pentane, etp = bis[3-(diphenylphosphino)ethyl]phenylphosphine. [b] Relative to external 85% H_3PO_4 in acetone-d_6. [c] Relative to external 85% H_3PO_4. [d] Reference 18a, relative to external 2 M aqueous K_2MoO_4. [e] Reference 18b, relative to external 2 M aqueous Na_2MoO_4. [f] Reference 8f, relative to saturated $Mo(CO)_6$ in THF. [g] Reference 18c, relative to 2 M aqueous K_2MoO_4. [h] Reference 14, relative to $W(CO)_6$ in CH_2Cl_2. [i] Nearly 11 signals, the three strongest were selected. [k] Relative to external 1.2 M Na_2PtCl_6 in D_2O. [l] Triplet, $^2J_{P-P}$ = 4 Hz, PPh. [m] Doublet, $^2J_{P-P}$ = 4 Hz, PPh_2.

chelate ring in the temperature range 193–303 K (Table I). In the case of **2** and **3**, they are flanked by satellites at $\pm^1/_2$ ($^1J_{M-P}$) arising from scalar coupling to the 14% abundant ^{183}W (**2**) or the 33% abundant ^{195}Pt nuclei (**3**). Because of fast quadrupolar relaxation processes, couplings to $^{95/97}Mo$ (16 and 9% natural abundance) are not visible in ^{31}P solution NMR spectra of compounds **1** and **4**. The positions of the ^{31}P signals agree with the values reported previously for **1a–d**,[8f,14] **2a–d**,[14] **3a–c**,[15] and **4**[8f] and correspond to the trend known for other bis(phosphine) chelate complexes:[8,15,16] in the four-membered chelate complexes **1a–3a** the phosphorus resonates at highest field, whereas the resonances of five-membered rings **1b–3b** are observed at lowest field (Table I, Figure 1). The signals of six- (**1c–3c**) and higher-membered rings (**1d–3d**, **1e–3e**) are positioned in between these two extrema, with that of **1c–3c** slightly at higher field compared to that of **1d–3d** and **1e–3e**. The differences between the chemical shifts of four- and five-membered rings are −54 (**1a,b**), −64 (**2a,b**), and −110 ppm (**3a,b**) and between five- and six-membered rings 34 (**1b,c**), 40 (**2b,c**), and 51 ppm (**3b,c**). Thus they show an additional dependence on the metal fragment attached to phosphorus in these complexes.

One phosphorus nucleus in compound **4** is involved into two chelate rings and is shifted to lower field by nearly twice the normal ring contribution. This demonstrates that the ring contribution is additive.[1b,17] The remaining two ^{31}P nuclei in compound **4** are involved in one chelate ring only and exhibit the same chemical shift as in compound **1b**.

The chemical shift data δ(M) for the center metal of the tungsten[14] and the molybdenum complexes[8f,18] were reported earlier by other authors (Table I). To complete these data, we recorded the $^{195}Pt\{^1H\}$ NMR spectra of compounds **3a–e**. They show a triplet due to coupling to ^{31}P of the bis(phosphines). In all three series **1–3** the metals in the four- to six-membered chelate rings experience a chemical shift opposite to that observed for δ(^{31}P) (Figure 1): in the four-membered chelates **1a–3a** the metals are deshielded, whereas the metals in the five-

(14) (a) Andrews, G. T.; Colquhoun, I. J.; McFarlane, W. *Polyhedron* **1983**, *2*, 783. (b) Coupling constants $^1J_{P-C}$ or sum of coupling constants $N = {}^1J_{P-C} + {}^3J_{P-C}$ (Hz) reported for **2a–d**:[14a] **2a** *N* 42.3 (ipso; this work $^1J_{P-C}$ 34.3, $^3J_{P-C}$ 9.1), 24.4 (α-CH_2); **2b** *N* 39.0 (ipso; this work $^1J_{P-C}$ 38.5, $^3J_{P-C}$ 1.7), 27.3 (α-CH_2); **2c** 38.5 (ipso), 24.3 (α-CH_2); **2d** 37.9 (ipso), 22.2 (α-CH_2).

(15) Appleton, T. G.; Bennett, M. A.; Tomkins, I. B. *J. Chem. Soc., Dalton Trans.* **1976**, 439.

(16) (a) Bechthold, H.-C.; Rehder, D. *J. Organomet. Chem.* **1981**, *206*, 305. (b) Bechthold, H.-C.; Rehder, D. *Ibid.* **1982**, *233*, 215. (c) Kelly, R. D.; Young, G. B. *Polyhedron* **1989**, *8*, 433.

(17) Meek, D. W.; Mazanec, T. J. *Acc. Chem. Res.* **1981**, *14*, 266.

(18) (a) Alyea, E. C.; Somogyvari, A. *Magn. Reson. Chem.* **1986**, *24*, 357. (b) Masters, A. F.; Bossard, G. E.; George, T. A.; Brownlee, R. T. C.; O'Connor, M. J.; Wedd, A. G. *Inorg. Chem.* **1983**, *22*, 908. (c) Alyea, E. C.; Lenkinski, R. E.; Somogyvari, A. *Polyhedron* **1982**, *1*, 130.

membered rings **1b–3b** are shielded. This antiparallel behavior was also reported for other bis(phosphine) complexes containing ^{51}V,[8e,16a] ^{93}Nb,[8e,16a,b] and ^{195}Pt.[8b,16c] In larger than six-membered rings this antiparallel trend vanishes.

With exception of the molybdenum complexes **1a–d** the coupling constants $^1J_{M-P}$ behave the same way as $\delta(^{31}P)$ (cf. Figure 1). In the case of the molybdenum compounds **1a–d** and **4** the one-bond coupling constants are too insensitive to structural changes and the reported[8f,18] experimental data obtained from ^{95}Mo NMR spectra deviate too much from each other to draw any conclusions. The one-bond coupling constants $^1J_{P-C}$ show no systematic variations in the $^{13}C\{^1H\}$ NMR spectra of compounds **2a–e**.[14] One might recognize a maximum value in the spectra of the five- and six-membered chelates **2b,c**.

Regarding the solution NMR data and reviewing other publications,[6] we make the following statements: (a) the ring effect in NMR spectra of organometallic compounds seems to be a general phenomenon, (b) the ring effect is clearly visible in $\delta(^{31}P)$, $\delta(M)$, and $^1J_{M-P}$ data of four- to six-membered rings, (c) the ring effect disappears in larger than six-membered rings, and (d) the complexes investigated in this paper show no exceptional behavior, and thus they are suitable as model compounds.

In the solid state, a distorted distribution of the electrons around the nucleus under observation causes a dependence of the chemical shift on the orientation of the molecule with respect to the external magnetic field. The solid-state spectrum of a stationary powdered sample therefore shows a broad feature, with the singularities (shoulders and peak) of this powder pattern (cf. Figure 5c,d) corresponding to the principal elements of the chemical shift tensor, δ_{ii} (i = 1–3).[10] In this notation the components δ_{ii} are given as chemical shifts with respect to a reference and δ_{11} and δ_{33} denote the least shielded and most deshielded principal components, respectively. Magic-angle spinning (MAS) at rotating speeds much below the powder line width causes the pattern to break up into a sharp isotropic line $\delta_{iso}(\text{solid}) = {}^1/_3(\delta_{11} + \delta_{22} + \delta_{33})$, flanked by spinning sidebands (cf. Figure 5b, dark peaks). The intensities of the spinning sidebands are related to the CSA and provide an opportunity to recover the anisotropy parameters by graphical analysis.[19]

The solid-state isotropic chemical shifts in the ^{31}P CP/MAS spectra of compounds **1–4** are summarized in Table I. In most cases the spectra exhibit two different signals with equal intensities, which indicate two crystallographically inequivalent phosphorus nuclei within the molecule or within the unit cell.[20] The crystal structures of **1a**,[21a] **1b**,[21b] **1c,d**[21c], **3b**,[21d] **3c**,[21e] and **3e**[21f] were reported previously. Although both phosphorus nuclei within the molecules are located in similar environments, they cannot be transformed into each other by a C_2 axis (**1b**, **3b**) or a mirror plane (**1a**), because there exist differences in corresponding M–P–C and C–P–C bond angles of 0.7–1.2 (**1a**),[21a] 0.3–2.0 (**1b**),[21b] and 0.1–4.2° (**3b**).[21d] Such small differences in geometry produce two well-resolved signals with separations of 5.7 (**1a**), 4.3 (**1b**), and 7.4 ppm (**3b**), which demonstrate the sensitivity of the chemical shift.

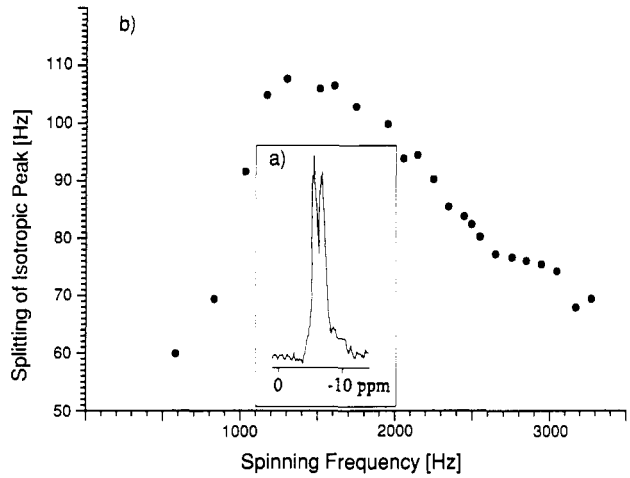

Figure 2. Dependence of the splitting of the center peak on the spinning frequency in the ^{31}P CP/MAS spectra of compound $(OC)_4W(dppp)$ (**2c**): (a) center peak in the ^{31}P CP/MAS spectrum at 1.3-kHz spinning frequency; (b) spinning rate dependence of the splitting.

In the ^{31}P CP/MAS spectra of the six-membered complexes **1c–3c**, however, we observed two overlapping signals (cf. Figure 2a). The splittings between these two signals are dependent on the spinning rate, depicted in Figure 2b for **2c**. Very recently, Kubo and McDowell[22] reported a similar behavior in the ^{31}P CP/MAS spectra of $Na_4P_2O_7{\cdot}10H_2O$. They proved that this effect is due to dipolar homonuclear coupling between spins with the same isotropic shift but different orientations of the chemical shift tensors. We observed an analogous spinning frequency dependence for **2c**: from the maximum value of 107 Hz at approximately 1.3 kHz the splitting decreases very rapidly, when the rotation rate was lowered. The splitting decreases slowly when the spinning frequency was increased. At twice the field strength (9.6 T, 162-MHz ^{31}P resonance frequency), the separation increases only by a factor of 1.5 and thus excludes a difference in the chemical shifts as the origin of the splitting.[22] From this behavior we concluded that the phosphorus nuclei in the six-membered rings **1c–3c** are related by symmetry but with different orientations of the chemical shift tensors within the molecule, in contradiction[23] with the results of the crystal structure determination for **3c**.[21de] It must be recognized that the X-ray data result from one crystal only and that polymorphism is quite common.[24] Therefore we carried out a powder X-ray diffraction experiment for **3c** using a scintillation counter. The 2θ values calculated from the reported triclinic cell dimensions[21e] are not consistent with our observed 2θ values. A good fit was obtained with a monoclinic unit cell, as was reported for $(SCN)_2Pd(dppp)$,[25] in which both phosphorus nuclei are related by a crystallographic C_2 axis.

For **2c** a single-crystal X-ray diffraction structure determination was carried out. There is difficulty in the refinement behavior of the crystal structure analysis.[26] A Patterson map placed the tungsten atom at a special position (0, 0.1445, 0), which means the two phosphorus

(19) Herzfeld, J.; Berger, A. E. *J. Chem. Phys.* **1980**, *73*, 6021.
(20) Clayden, N. J. *Chem. Scr.* **1988**, *28*, 211.
(21) (a) Cheung, K. K.; Lai, T. F.; Mok, K. S. *J. Chem. Soc. A* **1971**, 1644. (b) Bernal, I.; Reisner, G. M.; Dobson, G. R.; Dobson, C. B. *Inorg. Chim. Acta* **1986**, *121*, 199. (c) Ueng, C.-H.; Hwang, G.-Y. *Acta Crystallogr.* **1991**, *C47*, 522. (d) Farrar, D. H.; Ferguson, G. J. *Crystallogr. Spectrosc. Res.* **1982**, *12*, 465. (e) Robertson, G. B.; Wickramasinghe, W. A. *Acta Crystallogr.* **1987**, *C43*, 1694. (f) Klein, H.-P.; Thewalt, U.; Zettlmeissl, H.; Brune, H. A. Z. *Naturforsch.* **1981**, *36B*, 1125.
(22) Kubo, A.; McDowell, C. A. *J. Chem. Phys.* **1990**, *92*, 7156.
(23) The conformation of **3c** is similar to that of **2d**, if atom C6 is removed and a bond is formed between C5 and C7 instead.
(24) Fyfe, C. A. *Solid State NMR for Chemists*; CFC Press: Guelph, Ontario, Canada, 1983; p 377.
(25) Palenik, G. J.; Mathew, M.; Steffen, W. L.; Beran, G. *J. Am. Chem. Soc.* **1975**, *97*, 1059.
(26) Data: formula $C_{31}H_{28}O_4P_2W$; fw 708.35; space group $Pmn2_1$; a = 2197.7 (2) pm; b = 841.6 (1) pm; c = 772.3 (1) pm; $V = 1428.4 \times 10^6$ pm^3; Z = 2; d_{calcd} = 1.647 g cm^{-3}.

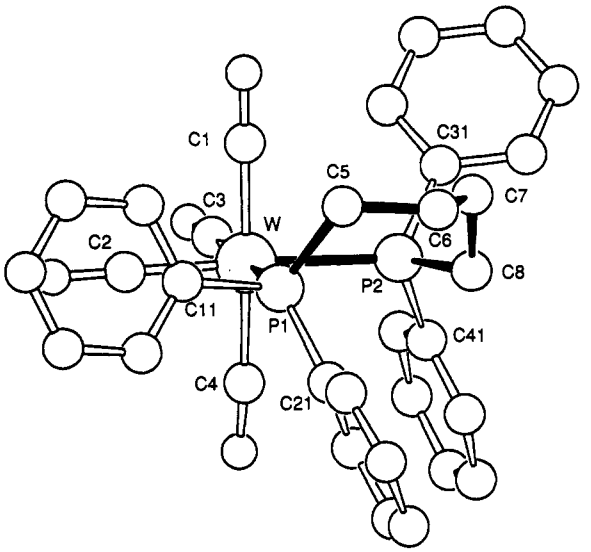

Figure 3. Molecular structure of compound $(OC)_4W(dppb)$ (**2d**).

atoms are crystallographically equivalent. Similar results were reported for the X-ray diffraction structure determination of **1c** with an exact mirror molecular symmetry through Mo, the two trans carbonyl groups, and the carbon in the middle of the backbone.[21c] This confirms the interpretation of the spinning frequency dependent splittings in the ^{31}P CP/MAS spectra of **1c–3c** as due to dipolar interactions between equivalent nuclei.

In the ^{31}P CP/MAS spectrum of the four-membered chelate **3a** we observed a similar spinning frequency dependent splitting as with the six-membered rings **1c–3c**. With a maximum value of 260 Hz at 2 kHz the splitting is much larger because of (a) the shorter P–P distance in four-membered rings (260–280 pm compared to 320–340 pm in six-membered rings) and (b) because of the larger chemical shift anisotropy[22] (vide infra).

As indicated by the calculated difference δ_{iso}(solid) – δ(soln) in Table I, the isotropic chemical shifts in the ^{31}P CP/MAS spectra of compounds 1–4 correspond to the chemical shifts in solution. These differences are often smaller than 3 ppm, especially in the smaller rings; in some larger rings, however, they may reach up to 18 ppm. As in the case of **3d** and **3e**, the mean values for the observed different chemical shifts achieve the values obtained from solution spectra. This may be due to different conformations, which are frozen in the solid state but averaged in solution. One example is the seven-membered ring **2d**, which exhibits two peaks separated by 10 ppm in its ^{31}P CP/MAS spectrum (Table I). Therefore we carried out an X-ray diffraction single-crystal structure determination for this compound. The two phosphorus nuclei are not equivalent (Figure 3), the P2–C(ring) bond is in the same plane as W and P1, whereas the P1–C(ring) bond is tilted away from the C8–P2–W–P1 plane. This difference in conformation between the two phosphorus atoms is especially manifested in the W–P–C(phenyl) angles which differ by about 5°, whereas the endocyclic W–P–C(ring) angles differ only within 1° (Table II). Analogous results were obtained from the single-crystal X-ray diffraction experiments on the isostructural molybdenum complex **1d**.[21c]

The one-bond coupling constants $^1J_{M-P}$ (M = $^{95/97}$Mo, ^{183}W, ^{195}Pt) were resolved in most cases and could be obtained from the ^{31}P CP/MAS spectra (Table I). Within the limits of error these values are similar to those obtained in solution. In the cases of the molybdenum and tungsten complexes, the changes again are too small to draw any conclusions. However, in the ^{31}P CP/MAS spectra of **3d** and **3e** we obtained two signals separated by 32 ppm in their isotropic chemical shifts and a difference of 400 Hz in their $^1J_{Pt-P}$ coupling constants. Because **3d** and **3e** show a behavior in their chemical shifts similar to **1d** and **2d**, we assume comparable structures.

Discussing the relationships between chemical shift and structure, one has to account for the three-dimensional nature of the chemical shift. The isotropic chemical shifts obtained from solution and from CP/MAS spectra are only averaged measures of changes in the electron distribution around the nuclei, structural effects, however, are amplified in the tensor components of the chemical shift anisotropy.[27]

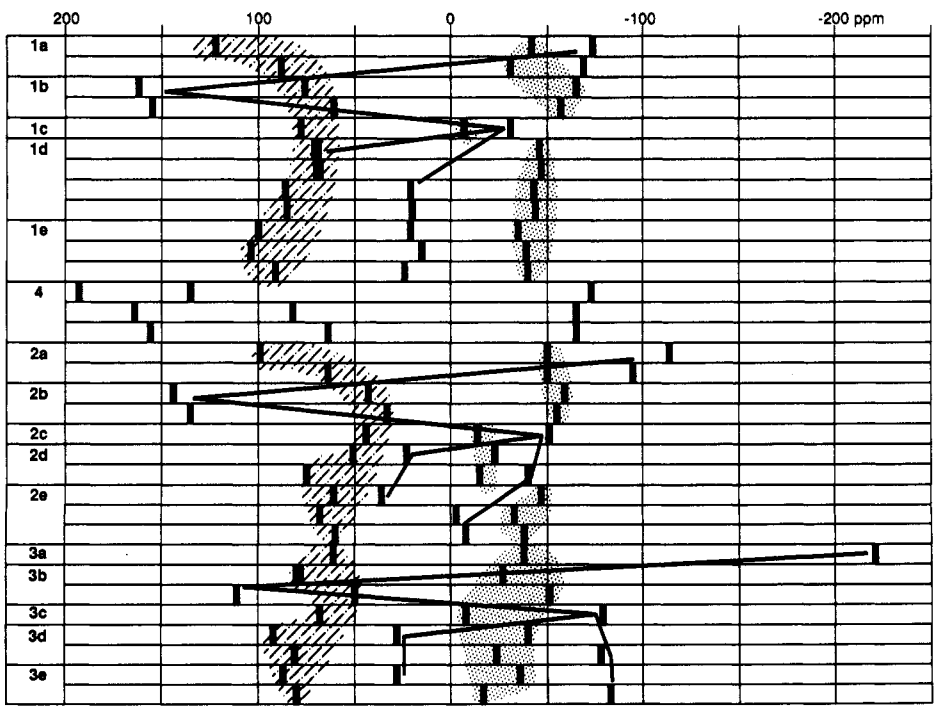

Figure 4. Observed stick spectra of the ^{31}P NMR chemical shift tensor principal components of compounds 1–4. Assignment is according to Figure 6: δ_{AA} (dotted area), δ_{BB} (lined area), and δ_{CC} (lines).

Table II. Selected Interatomic Distances (Å) and Angles (deg) for 2d with Estimated Standard Deviations in Parentheses

	Bond Lengths		
W–P1	2.537 (2)	C3–O3	1.165 (5)
W–P2	2.505 (2)	C4–O4	1.168 (5)
W–C1	1.994 (5)	P1–C5	1.854 (4)
W–C2	1.975 (5)	P1–C11	1.829 (4)
W–C3	1.967 (4)	P1–C21	1.823 (4)
W–C4	2.014 (5)	P2–C8	1.829 (4)
C1–O1	1.161 (5)	P2–C31	1.842 (4)
C2–O2	1.162 (5)	P2–C41	1.823 (5)
	Bond Angles		
P1–W–P2	91.73 (3)	W–P1–C21	124.0 (1)
P1–W–C1	84.2 (1)	C5–P1–C11	100.3 (2)
P1–W–C2	89.4 (1)	C5–P1–C21	101.2 (2)
P1–W–C3	175.1 (1)	C11–P1–C21	102.8 (2)
P1–W–C4	97.6 (1)	W–P2–C8	115.6 (1)
P2–W–C1	92.4 (1)	W–P2–C31	119.2 (1)
P2–W–C2	177.0 (1)	W–P2–C41	111.8 (1)
P2–W–C3	92.0 (1)	C8–P2–C31	102.2 (2)
P2–W–C4	88.5 (2)	C8–P2–C41	104.9 (2)
W–P1–C5	116.6 (1)	C31–P2–C41	101.4 (2)
W–P1–C11	108.8 (1)		

Therefore, we determined the principal values of the chemical shift tensors for compounds **1–4** (Table III, Figure 4). The tensor component scale covers a range from −221 (**3a**) to 193 ppm (**4**) compared to the isotropic chemical shifts, which vary from −66 (**3a**) to 85 ppm (**4**). Thus they define the local environment of the nuclei more exactly. This is particularly true when the principal axes system can be located in the molecular frame, which can be done properly only by single-crystal NMR investigations.[28] Nevertheless, in the cases of compounds **1–4** we want to apply several arguments to develop a rough picture about the orientation of the chemical shift tensor in such molecules.

A single-crystal NMR study carried out for the Wilkinson catalyst $ClRh(PPh_3)_3$ yielded three distinct chemical shift tensors for the three inequivalent sites.[29] In each case the most shielded component δ_{33} was directed along the metal–phosphorus bond. The values reported for δ_{33} of the phosphines trans to each other are close to the values we obtained from the CP/MAS spectra of compounds **1b,d,e–3b,d,e** and **4**; hence we assume the same orientation. A test for the validity of this assumption is possible if one realizes that the paramagnetic component of the tensor component is sensitive to changes in the plane perpendicular to it. Thus a change of the metal in isostructural complexes should affect the components perpendicular to δ_{33}.[11] A comparison of the tensor components obtained for **1b–3b** shows that δ_{11} and δ_{22} are altered by 20–70 ppm, whereas δ_{33} remains constant within the limit of errors. In the ^{31}P CP/MAS spectra of the four- and six-membered chelates **1a–3a** and **1c–3c**, however, δ_{22} is the component which does not change, while δ_{11} and δ_{33} vary 40–50 ppm. This apparent change is because the nomencleature δ_{ii} (i = 1–3) follows the order of the components in the spectrum and is not related to the orientation of the shift tensor within the molecule. Thus, i.e., the value of δ_{22} for **2a** (−50 ppm) is very close to that of δ_{33} for **2b** (−55 and −59 ppm) and it is reasonable to assume the same orientation for these tensor components.

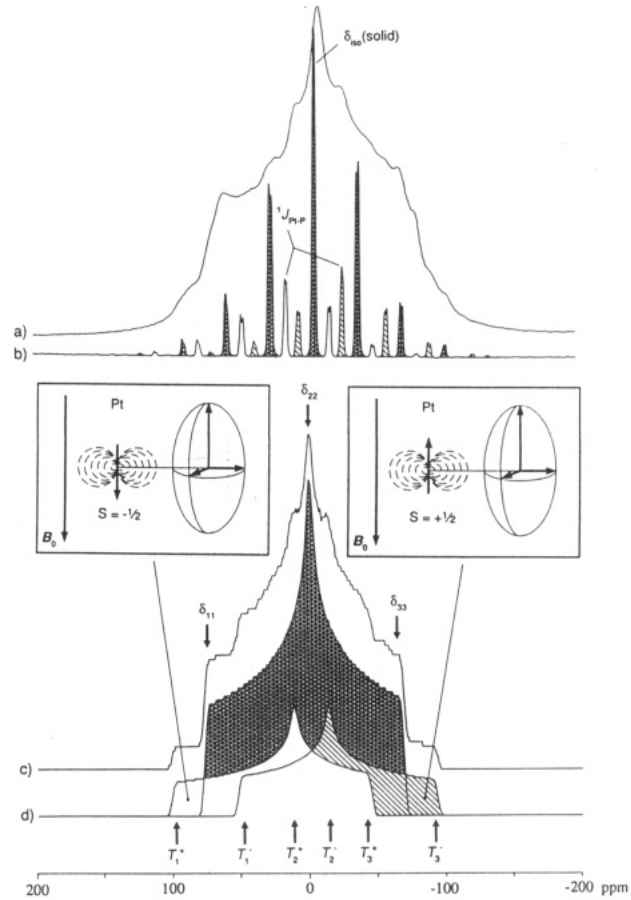

Figure 5. Observed ^{31}P CP spectra of $Cl_2Pt(dppp)$ (**3c**) at 81 MHz with proton dipolar decoupling: (a) static powder pattern; (b) sample spinning at the magic angle with 2580-Hz rotor frequency, dark peaks correspond to nonsatellite peaks, lined and white peaks are related to the $+^1/_2$ and $-^1/_2$ subspectra, respectively; (c) simulated static powder shape; (d) subspectra of the simulated powder pattern, showing the principal components of the composite tensor **T**.

In certain cases it is possible to define the orientation of some of the shielding components by using the dipolar interaction which is fixed by the molecular geometry.[30] In the CP/MAS spectra of compounds **3**, the sideband patterns of the nonsatellite ^{31}P NMR resonances reflect only the principal values of the anisotropic part of the ^{31}P chemical shift tensor δ (Figure 5b,d, dark peaks). The patterns of the satellites depend on the principal values of a composite tensor **T** which contains chemical shift anisotropy δ and dipolar direct (**D**) and scalar indirect coupling (**J**), as well as their relative orientations.[31] For one spin state of ^{195}Pt, the dipolar and shift anisotropy interactions reinforce each other, whereas for the other one, they partially cancel, resulting in different effective anisotropies for the two satellite subspectra $S = +^1/_2$ and S

(27) (a) Dutasta, J. P.; Robert, J. B.; Wiesenfeld, L. *Chem. Phys. Lett.* **1981**, *77*, 336. (b) Tullius, M.; Lathrop, D.; Eckert, H. *J. Chem. Phys.* **1990**, *94*, 2145. (c) Curtis, R. D.; Penner, G. H.; Power, W. P.; Wasylishen, R. E. *J. Phys. Chem.* **1990**, *94*, 4000. (d) Grimmer, A.-R.; Neels, J. Z. *Anorg. Allg. Chem.* **1989**, *576*, 117. (e) Carty, A. J.; Fyfe, C. A.; Lettinga, M.; Johnson, S.; Randall, L. H. *Inorg. Chem.* **1989**, *28*, 4120. (f) Zilm, K. W.; Webb, G. G.; Cowley, A. H.; Pakulski, M.; Orendt, A. *J. Am. Chem. Soc.* **1988**, *110*, 2032. (g) Penner, G. H.; Wasylishen, R. E. *Can. J. Chem.* **1989**, *67*, 1909.

(28) (a) Kohler, S. J.; Klein, M. P. *Biochemistry* **1976**, *15*, 967. (b) Gibby, M. G.; Pines, A.; Rhim, W.-K.; Waugh, J. S. *J. Chem. Phys.* **1972**, *56*, 991. (c) Marchetti, P. S.; Honkonen, R. S.; Ellis, P. D. *J. Magn. Reson.* **1987**, *71*, 294. (d) Igner, D.; Fiat, D. *Ibid.* **1982**, *46*, 233.

(29) Naito, A.; Sastry, D. L.; McDowell, C. A. *Chem. Phys. Lett.* **1985**, *115*, 19.

(30) (a) Power, W. P.; Wasylishen, R. E. In *Annual Reports on NMR Spectroscopy*; Webb, G. A., Ed.; Academic Press: London, 1991; Vol. 23, p 1. (b) Power, W. P.; Lumsden, M. D.; Wasylishen, R. E. *Inorg. Chem.* **1991**, *30*, 2997. (c) Haubenreisser, U.; Sternberg, U.; Grimmer, A.-R. *Mol. Phys.* **1987**, *60*, 151.

(31) (a) Harris, R. K.; Packer, K. J.; Thayer, A. M. *J. Magn. Reson.* **1985**, *62*, 284. (b) Zilm, K. W.; Grant, D. M. *J. Am. Chem. Soc.* **1981**, *103*, 2913.

Table III. Calculated ^{31}P NMR Chemical Shift Anisotropy Parameters[a] for Compounds 1–4[b]

compd	no.	δ_{11}	δ_{22}	δ_{33}	$\Delta\delta$[c]	ρ,[d] %	no. of spinning rates
$(OC)_4Mo$(dppm)	**1a**	122 (2)	−42 (5)	−74 (6)	196	−67	3
		88 (1)	−31 (3)	−69 (3)	157	−52	
$(OC)_4Mo$(dppe)	**1b**	162 (3)	76 (2)	−65 (3)	227	24	4
		155 (1)	61 (3)	−57 (3)	212	11	
$(OC)_4Mo$(dppp)	**1c**	78 (2)	−7 (2)	−31 (1)	109	−56	4
$(OC)_4Mo$(dppb)	**1d**	71 (1)	71 (1)	−46 (2)	117	100	3
		70 (1)	70 (1)	−47 (2)	117	100	
		86 (3)	21 (2)	−43 (2)	129	0	
		85 (3)	20 (2)	−44 (2)	129	0	
$(OC)_4Mo$(dpppe)	**1e**	100	21	−35	135	−17	2
		104	15	−39	143	−24	
		91	24	−40	131	−2	
$(OC)_4W$(dppm)	**2a**	99 (3)	−50 (5)	−114 (1)	213	−40	4
		64 (1)	−50 (2)	−95 (1)	159	−43	
$(OC)_4W$(dppe)	**2b**	144 (1)	43 (1)	−59 (1)	203	0	5
		135 (1)	33 (1)	−55 (1)	190	−7	
$(OC)_4W$(dppp)	**2c**	44 (6)	−14 (10)	−51 (5)	95	−22	4
$(OC)_4W$(dppb)	**2d**	51 (3)	23 (5)	−23 (4)	74	24	4
		75 (1)	−15 (3)	−40 (3)	115	−57	
$(OC)_4W$(dpppe)[e]	**2e**	61 (1)	36 (1)	−47 (1)	108	54	3
		68 (1)	−3 (3)	−33 (3)	101	−40	
		60 (2)	−8 (6)	−38 (4)	98	−39	
Cl_2Pt(dppm)	**3a**	61 (2)	−38 (1)	−221 (2)	282	30	6
Cl_2Pt(dppe)	**3b**	80 (1)	80 (1)	−27 (2)	107	100	
		111 (1)	50 (1)	−51 (2)	162	25	
Cl_2Pt(dppp)	**3c**	68 (2)	−8 (2)	−79 (1)	147	−3	6
Cl_2Pt(dppb)	**3d**	92 (1)	28 (3)	−40 (2)	132	3	2
		81 (3)	−24 (3)	−78 (5)	159	−32	
Cl_2Pt(dpppe)	**3e**	87	28	−36	123	4	1
		80	−17	−83	163	−19	
fac-$(OC)_3Mo$(etp)	**4**	193 (2)	135 (4)	−73 (1)	266	56	3
		164 (1)	82 (2)	−65 (1)	229	28	
		156 (5)	64 (6)	−65 (2)	221	17	

[a] From graphical analysis of sideband intensities[19] or from singularities of the powder pattern; standard deviations in parentheses. [b] For abbreviations see Table I. [c] Anisotropy range $\Delta\delta = \delta_{11} - \delta_{33}$. [d] Asymmetry parameter $\rho = (\delta_{11} + \delta_{33} - 2\delta_{22})/(\delta_{33} - \delta_{11})$. [e] See Table I, footnote *i*.

$= -1/2$ (Figure 5b,d, white and lined pattern). If **J** is assumed to be axially symmetric and colinear with **D**, one is able to calculate the effective dipolar coupling constant $D' = D - (J_\parallel - J_\perp)/3$ from the composite tensor components T_i^+- and the angle ϕ (eq 1).[31]

$$\phi_{ij} = \tfrac{1}{2} \arccos [(\alpha^+)^2 - (\alpha^-)^2]/6\nu_a D' \qquad i, j, k = 1\text{–}3 \quad (1)$$

$$D' = T_k^+ - T_k^- - J = (T_i^- + T_j^-) - (T_i^+ + T_j^+) + 2J$$

$$\alpha^+ = T_i^+ - T_j^+$$

$$\alpha^- = T_i^- - T_j^-$$

$$\nu_a = \{\tfrac{1}{2}[(\alpha^+)^2 + (\alpha^-)^2 - 9(D')^2/2]\}^{1/2} = \delta_{ii} - \delta_{jj}$$

In the case of the six-membered ring **3c**, the calculated shift tensor components correspond within 40 Hz to the values obtained from the nonsatellite peaks. An effective dipolar coupling constant of $D' = 660$ Hz was obtained and the shift tensor component δ_{22} forms an angle of $\phi = 9°$ with the phosphorus–platinum bond. This confirms the assumption made above that for compounds **1c–3c** δ_{22} is directed mostly along the metal–phosphorus bond. Using the value of 223 ppm[21e,32] for the ^{195}Pt–^{31}P bond, we calculated the dipolar coupling constant $D = (\mu_0/4\pi)(\gamma_{Pt}\gamma_P/r_{Pt\text{-}P}^3)(h/4\pi^2)$ to be 940 Hz. The difference in the effective dipolar coupling constant D' is ascribed to a significant anisotropic **J** tensor ($\Delta J = 840$ Hz).[30,33] These results are in excellent agreement with a present dipolar/chemical shift NMR study on six platinum cis and trans complexes Cl_2PtL_2 (L = tertiary phosphine).[33e] In each case δ_{22} points along the Pt–P bond and ΔJ has values of 1000–2200 Hz.

Due to the unfavorable ratio $\delta/\mathbf{D} \approx 10$–15, which means the spectra are dominated by the chemical shift anisotropy, and the appearance of two distinct species, the exact evaluation of sideband intensities was restricted to **3a–c**. In the case of **3b** the effective dipolar coupling was calculated to be $D' = 390$ Hz for the species at $\delta_{iso} = 44.1$ ppm. Thus the anisotropy for the scalar coupling of ΔJ equals 1660 Hz. In this species the high-field component δ_{33} is directed toward the metal, as expected from the discussion above. In the ^{31}P CP/MAS spectrum of compound **3a** an effective dipolar coupling constant D' of ca. 230 Hz was determined, which indicates a larger anisotropy in scalar coupling ($\Delta J = 2130$ Hz). The ring strain leads to a deviation of 20–30° of δ_{22} from the proposed direction toward the platinum.

A basic assumption often applied in discussions about the orientation of tensor components is that changes in the environment of the phosphorus nuclei produce changes in the values of the principal components, leaving the orientation of the principal axes unaffected.[34] Because the nuclear spin is only sensitive to its local environment within two or three coordination spheres[20] the directions of the principal components of the shift tensors are basically dictated by the local symmetry of the PPh_2 group. Therefore the local mirror plane at phosphorus requires

(32) Hofmann, P.; Heiss, H.; Müller, G. *Z. Naturforsch.* **1987**, *42B*, 395.
(33) (a) Penner, G. H.; Power, W. P.; Wasylishen, R. E. *Can. J. Chem.* **1988**, *66*, 1821. (b) Santos, R. A.; Chien, W. J.; Harbison, G. S.; McCurry, J. D.; Roberts, J. E. *J. Magn. Reson.* **1989**, *84*, 357. (c) Balz, R.; Haller, M.; Hertler, W. E.; Lutz, O.; Nolle, A.; Schafitel, R. *Ibid.* **1980**, *40*, 9. (d) Grimmer, A.-R.; Peter, R.; Fechner, E. *Z. Chem.* **1978**, *18*, 109. (e) Power, W. P.; Wasylishen, R. E. Manuscript submitted for publication.

(34) (a) Barra, A. L.; Robert, J. B. *Chem. Phys. Lett.* **1987**, *136*, 224. (b) Jagannathan, N. R. *Magn. Reson. Chem.* **1989**, *27*, 941. (c) VanderHart, D. L. *J. Chem. Phys.* **1976**, *64*, 830.

Table IV. Mean Geometries[a] at Phosphorus for Different Ring Sizes[b]

		P-M-X	M-P-C	M-P-R^1	M-P-R^2	C-P-R^1	C-P-R^2	R^1-P-R^2
four-membered rings	mean	71.1	94.6	121.2	119.5	107.6	106.9	104.8
	σ_d[c]	3.0	1.2	3.1	4.2	2.0	2.2	3.3
	min	66.1	91.8	116.4	111.0	103.3	101.4	97.2
	max	76.3	97.5	127.1	127.1	109.7	110.4	110.9
	$\sum$M-P-C/R		335.3					
	$\sum$C/R-P-R					319.3		
five-membered rings	mean	85.1	107.5	119.0	117.3	103.0	104.4	103.8
	σ_d[c]	3.1	1.9	3.9	3.6	3.0	2.1	3.8
	min	80.2	103.3	110.1	110.5	97.1	99.7	97.8
	max	90.8	111.2	127.4	124.5	111.2	111.6	111.9
	$\sum$M-P-C/R		343.8					
	$\sum$C/R-P-R					311.2		
six-membered rings	mean	89.3	114.6	114.5	115.9	101.5	104.2	104.4
	σ_d[c]	3.8	2.5	3.0	3.8	2.3	2.0	3.3
	min	85.1	108.9	109.3	110.1	96.6	99.2	99.1
	max	99.1	120.2	123.2	107.2	107.3	112.1	56.0
	$\sum$M-P-C/R		345.0					
	$\sum$C/R-P-R					310.1		
seven-membered rings	mean	97.6	117.5	113.0	117.5	102.3	101.0	102.0
	σ_d[c]	4.5	2.9	2.1	2.9	3.2	2.8	2.6
	min	90.3	111.0	108.8	113.8	95.3	94.3	96.3
	max	106.1	123.2	116.4	124.0	107.0	107.5	104.2
	$\sum$M-P-C/R		348.0					
	$\sum$C/R-P-R					305.3		
acyclic compds	mean	98.1	112.1	114.8	118.7	100.7	103.2	105.3
	σ_d[c]	2.1	2.1	2.1	2.5	2.3	1.8	2.4
	$\sum$M-P-C/R		345.6					
	$\sum$C/R-P-R					309.2		

[a] 20–40 entries for each type. Included are also monophosphine complexes and substituents other than phenyl groups. Full data tables are available from the authors. [b] In chelate systems P-M-X describes the endocyclic angle at the center metal, R^1 and R^2 stand for equatorial and axial substituents, respectively. In acyclic systems P-M-X is the angle to the nearest neighbor and M-P-C, M-P-R^1, and M-P-R^2 are sorted for each phosphine for increasing magnitude. [c] Standard deviation.

one component perpendicular to this plane. The three α-carbon atoms neighboring the phosphorus lead to a local C_3 axis and demand one of the tensor components directed along this axis. In the spectra of the five-membered chelates **1b–3b** δ_{33} corresponds to this component, whereas in the spectra of the four- and six-membered rings **1a–3a** and **1c–3c** δ_{22} is related to this orientation. For the sake of convenience we want to change to the nomenclature δ_{ii} (i = A, B, C) when considering the orientation of a shift tensor component. Thus δ_{AA} is oriented along the local C_3 axis, which points in most cases to the metal (Figure 6), and shows no systematic variations with the ring size (dotted area in Figure 4). We assume that the in-plane tensor component perpendicular to δ_{AA} corresponds to δ_{11} and we label this in-plane component δ_{BB} (Figure 6). δ_{BB} exhibits a systematic dependence on the ring size (Figure 4, lined area) with a minimum value in the five- or six-membered chelates.

The remaining component δ_{CC} perpendicular to the mirror plane (Figure 6) shows the largest variation with the ring size (Figure 4), as established for ^{13}C shift tensors in cycloalkanes.[35] Thus δ_{CC} covers a range of 400 ppm and is related to δ_{11}, δ_{22}, or δ_{33}. This component determines the behavior of the isotropic shift. Concluding the assignments of principal components to specific orientations, we can state that each of the shift tensor components shows a different dependence on the ring size.

To get a more extensive data base for structural considerations, reported crystal structures of chelate and acyclic compounds are collected and summarized in Table IV.[36] The only structural parameter which shows a distinct dependence on the ring size is the endocyclic M-P-C angle. This is not unexpected, but attempts for the systematization of this influence have been less than successful hitherto.[37] The endocyclic M-P-C angle opens continuously from 95° in four-membered cycles to 118° in seven-membered rings (Table IV). The five-membered chelates have M-P-C angles close to the tetrahedral angle. Their resonances are at lowest field compared to the spectra of other ring sizes;[6] thus any deviation from the tetrahedral angle, squeezing or stretching, causes an upfield shift. The mean values given in Table IV represent to a good approximation the geometry of "standard" rings in solution. Combined with the solution shift data the following bond angle dependencies were calculated. The endocyclic M-P-C angle of the standard four-membered ring is 13° smaller and that of the six-membered cycle 7° larger than that of the five-membered counterpart. This causes in the solution spectra of the four- and six-membered complexes an upfield shift of 4 (**1a**) and 5 ppm/deg

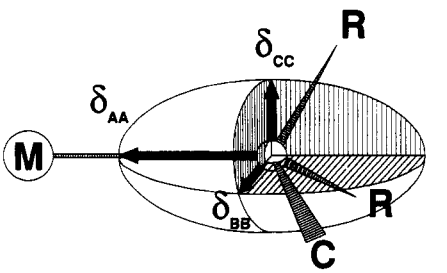

Figure 6. Assignment of the principal values of the chemical shift tensor of phosphorus to specific orientations within the molecular framework of compounds **1–3**. δ_{AA} points along the local C_3 axis toward the metal, δ_{BB} is located in the mirror plane defined by M, P, and C, δ_{CC} is oriented pependicular with respect to this plane.

(35) (a) Facelli, J. C.; Orendt, A. M.; Beeler, A. J.; Solum, M. S.; Depke, G.; Malsch, K. D.; Downing, J. W.; Murthy, P. S.; Grant, D. M.; Michl, J. *J. Am. Chem. Soc.* **1985**, *107*, 6749. (b) Facelli, J. C.; Grant, D. M. In *Topics in Stereochemistry*; Eliel, E. L., Wilen, S. H., Eds.; John Wiley and Sons: New York, 1989; Vol. 19, p 1.

(36) The full data tables are available from the authors.

(37) Gallagher, M. J. In ref. 1a, p 297.

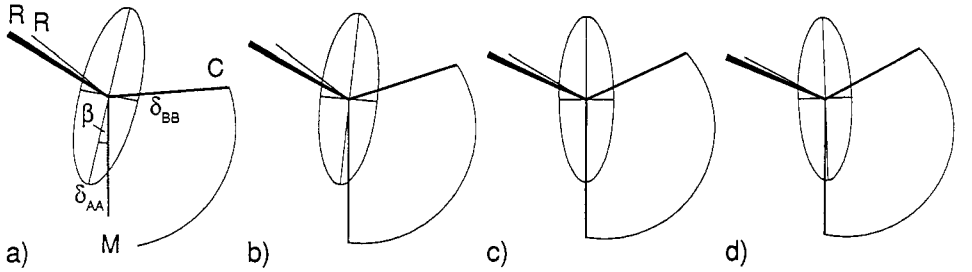

Figure 7. Tilting of the ^{31}P chemical shift tensor in four- (a) to seven-membered (d) chelates according to the bond angles given in Table IV.

(**1c**) for molybdenum, of 5 (**2a**) and 6 ppm/deg (**2c**) for tungsten, and of 8 (**3a**) and 7 ppm/deg (**3c**) for platinum. There seems to be a relative constant slope within one series and this range of the bond angle, with the slope for the heavier metals being steeper. The standard deviations in Table IV indicate that the endocyclic M–P–C angles are restricted to narrow ranges for each ring size. Hence the error should be small if these angles are used to calculate the bond angle dependence of δ_{CC} in the ^{31}P CP/MAS spectra of compounds **3a–c**. Compared to that of the spectrum of **3b** δ_{CC} is shifted 330 ppm to higher field in the spectrum of **3a**, with 25 ppm/deg, and in that of **3c** about 190 ppm, with 27 ppm/deg. Similar nonmonotonic variations of $\delta(^{31}P)$ with bond angle changes were reported for other phosphorus compounds,[38] and theoretical calculations for PH_3 showed a minimum of shielding near 110° for the component $\sigma_\perp$ on variation of the H–P–H angle.[2b]

This simple picture upon a relation between chemical shift and deviation from the tetrahedral angle seems to fail if larger than six-membered rings were included. Although they have larger endocyclic bond angles (Table IV), their signals are shifted back to lower field compared to the six-membered rings (Figure 1). In a tetracoordinated species six bond angles are necessary to describe the structure. If one angle changes, the other angles have to open and to close in a complementary manner and the ring effect must be treated as a complex interplay of several bond angles. The angles given in Table IV indicate that changes in the endocyclic M–P–C angles are mainly reflected in the two M–P–R angles. As a net result of the various angular changes the substituents R are moved toward the other coordination sites of the metal if the M–P–C angle is increased.[39] This rationalization corresponds to the concept of bond bending described by Powell[40] and visualizes the stereochemical features of the different ring sizes. In this concept only the three α-carbon atoms are included and the tilt angle β is considered as a deviation of the C_3 axis of the P(α-C)$_3$ unit from the M–P axis (Figure 7).

Using this description, one is able to explain the different behaviors of the tensor components δ_{AA} and δ_{CC}. The data in Table IV show that the angles within the P(α-C)$_3$ unit experience the smallest changes on variations of the ring size. The component δ_{AA} sensitive for changes within this unit is directed along the C_3 axis and shows the smallest variations in the spectra of compounds **1–4**. Their magnitudes cover the range between –10 and –60 ppm, and even the values for square-planar complexes of rhodium[29] and platinum,[33e] for octahedral complexes of manganese,[11] and for piano-stool complexes of tungsten and molybdenum[11] fall within this range. In the four-membered chelates the tilting of the M–P bond causes a deviation of δ_{AA} from the M–P axis (Figure 7a); therefore none of the components is directed toward the metal, as shown for **3a** by dipolar NMR spectroscopy. The component δ_{CC} perpendicular to the ring plane is sensitive for the combined changes of the endocyclic M–P–C and exocyclic M–P–R angles. Values of these angles close to the tetrahedral value lead to a deshielding contribution for this shift tensor component.

The influence of symmetry on the sensitivity of the principal components is visible in the ^{31}P CP/MAS spectrum of the bicyclic complex **4**. Both Ph_2P groups are involved in one chelate system only, and their shift tensors correspond to those of **1b** (Figure 4). The PhP group, however, is part of two chelate systems. Hence $\delta(^{31}P)$ is shifted nearly twice the normal ring contribution to lower field. Because of the changed local symmetry, none of the tensor components δ_{BB} and δ_{CC} is perpendicular to the endocyclic Mo–P–C planes and the downfield shift is distributed to both tensor components.

Conclusions

The present work demonstrates the extraordinary sensitivity of the chemical shift and especially of the chemical shift tensor principal components on slight changes in structure. In the ^{31}P CP/MAS spectra of **3a–c** the calculated bond angle dependence of 25–27 ppm/deg for δ_{CC} is of 1 order of magnitude, not easily achieved by diffraction methods. Arguments based on symmetry, changes in the central metals, and the dipolar ^{195}Pt–^{31}P interaction allow us to propose a pictorial model about the orientation of the ^{31}P shift tensor within the molecular frame. In combination with mean bond angles at phosphorus for each ring size, this model visualizes the qualitative dependence of the shift tensor components on the stereochemical features of complexes **1–4**. The dependence of $\delta(^{31}P)$ on the ring size of four- to eight-membered chelates can be explained as a complex interplay of all bond angles at phosphorus, in which an angle close to the tetrahedral value leads to a downfield shift of the respective tensor component. In the ^{31}P CP/MAS spectra of compounds **3a–c** the bending of the Pt–P bond seems to cause a considerable anisotropy of the scalar coupling constant $^1J_{Pt-P}$. To establish a quantitative relation between $\delta(^{31}P)$ and changes in bond angles, very accurate single-crystal X-ray structure determinations and single-crystal NMR experiments for several homologous series of chelate complexes are necessary.

Experimental Section

General Procedures. The ligands were made as described elsewhere and were purified by recrystallization.[41] The complexes

(38) (a) Gorenstein, D. G. *J. Am. Chem. Soc.* **1975**, *97*, 898. (b) Martin, J.; Robert, J. B. *Org. Magn. Reson.* **1981**, *15*, 87.
(39) Palenik, G. J.; Mathew, M.; Steffen, W. L.; Beran, G. *J. Am. Chem. Soc.* **1975**, *97*, 1059.
(40) Powell, J. *J. Chem. Soc., Chem. Commun.* **1989**, 200.
(41) Colquhoun, I. J.; McFarlane, W. *J. Chem. Soc., Dalton Trans.* **1982**, 1915.

1, 2, and 4 were prepared by stirring stoichiometric amounts of the ligand and the appropriate metal hexacarbonyl in diglyme at 140 °C for 6 h, followed by removal of the diglyme in vacuo and recrystallization from CH_2Cl_2/*n*-hexane. The complexes **1e** and **2e** were mentioned previously in the literature,[42] but the IR data given are not consistent with a *cis*-$(OC)_4ML_2$ species. Complexes **3** were synthesized via the heterogenous reaction of the ligand with K_2PtCl_4 in dichloromethane.[21f] The product was purified by recrystallization from dichloromethane. Instrumentation: mass spectra, Finnigan MAT 711 A; IR spectra, Bruker FT-IR spectrometer, Model IFS 48; $^{13}C\{^1H\}$ NMR spectra, Bruker AC 250 at 62.9 MHz (with the exception of the axial CO groups and carbon atoms at central positions within the chelate, all signals form the A part of an AXX′ system, the low solubility restricted in the case of **1e** the evaluation of the splitting *N* of the principal doublet);[14] $^{31}P\{^1H\}$ NMR spectra Bruker WP 80 at 32.4 MHz. Elemental analyses were carried out with Carlo Erba Model 1106 and Perkin-Elmer Model 4000 atomic absorption spectrometers.

$(OC)_4Mo(dpppe)$ (1e). Molybdenum hexacarbonyl (1.41 g, 5.3 mmol) and dpppe (2.19 g, 5.0 mmol) were reacted: yield 0.68 g (21%); mp 189 °C dec; IR [ν(C≡O) (cyclohexane, cm^{-1})] 2021 (s), 1933 (s), 1904 (vs), 1901 (sh); $^{13}C\{^1H\}$ NMR (62.9 MHz, $CDCl_3$, 303 K) δ 138.99 (m, N = 33.4 Hz, C1, ipso carbons), 132.28 (m, N = 11.4 Hz, C2,6), 129.35 (s, C4), 128.30 (m, N = 8.4 Hz, C3,5), 29.67 (m, N = 17.2 Hz, PC), 25.77 (t, $^3J_{P-C}$ = 6.5 Hz, PCC*C*), 21.17 (s, PC*C*); MS (FD, 80 °C) *m/e* (relative to ^{98}Mo) 650. Anal. Calcd for $C_{33}H_{30}MoO_4P_2$: C, 61.16; H, 4.67; Mo, 14.73. Found: C, 60.97; H, 4.53; Mo, 14.32.

$(OC)_4W(dpppe)$ (2e). Tungsten hexacarbonyl (1.31 g, 3.7 mmol) and dpppe (1.50 g, 3.5 mmol) were reacted: yield 1.86 g (72%); mp 218 °C dec; IR [ν(C≡O) (cyclohexane, cm^{-1})] 2018 (s), 1927 (s), 1898 (vs), 1893 (vs); $^{13}C\{^1H\}$ NMR (62.9 MHz, $CDCl_3$, 303 K) δ 207.72 (m, $^2J_{P-C,trans}$ = 27.1, $^2J_{P-C,cis}$ = −8.0, $^2J_{P-P}$ = 18.9 Hz, CO_{eq}), 205.87 (t, $^2J_{P-C}$ = 6.7 Hz, CO_{ax}), 140.79 (m, $^1J_{P-C}$ = 37.8, $^3J_{P-C}$ = 2.3, $^2J_{P-P}$ = 20.6 Hz, C1, ipso carbons), 134.26 (m, N = 10.5 Hz, C2,6), 131.42 (s, C4), 130.14 (m, N = 8.6 Hz, C3,5), 30.41 (m, $^1J_{P-C}$ = 22.2, $^3J_{P-C}$ = −0.3, $^2J_{P-P}$ = 19.4 Hz, PC), 25.72 (t, $^3J_{P-C}$ = 5.7 Hz, PCC*C*), 21.46 (s, PC*C*); MS (FD, 80 °C) *m/e* (relative to ^{184}W) 736. Anal. Calcd for $C_{33}H_{30}O_4P_2W$: C, 53.82; H, 4.11; W, 24.97. Found: C, 53.90; H, 4.43; W, 24.31.

NMR Spectra. All solid-state spectra were recorded by using the standard accessory on a Bruker MSL 200 wide-bore spectrometer. The ^{31}P NMR spectra were recorded by using high-power proton decoupling and magic-angle spinning for line narrowing and cross polarization for sensitivity enhancement. The 90° ^{31}P pulse was 5.2 μs, and the contact time was varied between 0.5 and 40 ms. Optimum signal enhancements were achieved with a contact time of 2 ms. Referencing of the $\delta(^{31}P)$ scale was performed by using $\delta(H_3PO_4) = 0$ as external standard. Reported tensor components are mean values obtained from different measurements at spinning rates between 1.0 and 3.9 kHz. Numbers for these measurements are given in Table III. The standard deviations denote the scattering of these measurements. An absolute error of 5 ppm is estimated.

X-ray Structure Determination of 2d. Pale yellow crystals of **2d** were obtained by crystallization from dichloromethane/*n*-hexane. A suitable crystal with approximate dimensions 0.15 × 0.15 × 0.2 mm was mounted on a glass fiber and then transferred to an Enraf-Nonius CAD-4 diffractometer. The lattice constants were determined with 25 precisely centered high-angle reflections. The final cell parameters and specific data collection parameters for **2d** are summarized in Table V. A study on the diffractometer indicated a monoclinic crystal system, and systematic absences are consistent only with the space group $P2_1/n$ (No. 14). The structure was solved by standard Patterson methods,[43] and difference Fourier syntheses[44] were used to locate the remaining non-hydrogen atoms. The DIFABS[45] method of absorption correction was applied after isotropic refinement of all non-hydrogen atoms. The hydrogen atoms were placed at calculated positions and included in the structure factor calculation. Final atomic positional parameters for **2d** are listed in Table VI.

Table V. Crystal Data and Summary of Intensity Data Collection and Structure Refinement of 2d

formula	$C_{32}H_{28}O_4P_2W$
fw	722.38
space group	$P2_1/n$
a, pm	1202.8 (1)
b, pm	1531.8 (1)
c, pm	1654.1 (2)
β, deg	104.72 (1)
V, pm^3	2947.7 × 10^6
Z	4
d_{calcd}, g cm^{-3}	1.628
T, °C	−50
F(000), e	1424
μ(Mo Kα), cm^{-1}	41.43
λ(Mo Kα radiatn, graphite monochromator), Å	0.709 30
θ limits, deg	3–25
scan type	ω/θ
max scan time, s	40
h,k,l range	0 → 14,0 → 18,−19 → +19
no. of reflectns measd	3794
no. of unique data with $I \geq 3\sigma(I)$	4083
no. of variables	352
R	0.039
R_w	0.044
weighting scheme	$w^{-1} = \sigma^2(F)$

Table VI. Fractional Atomic Coordinates (Esd's in Parentheses) of 2d with Equivalent Isotropic Thermal Parameters U_{eq} (Å²)[a]

atom	*x*	*y*	*z*	U_{eq}
W	0.07726 (3)	0.23191 (2)	0.37394 (2)	0.025 (1)
P1	−0.0625 (2)	0.2268 (1)	0.4657 (1)	0.026 (1)
P2	0.2213 (2)	0.3154 (1)	0.4823 (1)	0.027 (1)
O1	−0.0577 (7)	0.4028 (5)	0.3009 (4)	0.065 (4)
O2	−0.0903 (6)	0.1187 (4)	0.2379 (4)	0.047 (4)
O3	0.2290 (6)	0.2388 (5)	0.2458 (4)	0.065 (5)
O4	0.2180 (6)	0.0581 (4)	0.4351 (5)	0.056 (4)
C1	−0.0078 (7)	0.3402 (6)	0.3282 (5)	0.034 (4)
C2	−0.0308 (7)	0.1609 (6)	0.2895 (5)	0.034 (4)
C3	0.1742 (7)	0.2377 (6)	0.2946 (5)	0.035 (4)
C4	0.1647 (7)	0.1220 (5)	0.4163 (5)	0.033 (4)
C5	−0.1117 (7)	0.3334 (5)	0.4970 (5)	0.033 (4)
C6	−0.0346 (7)	0.3797 (5)	0.5723 (5)	0.035 (4)
C7	0.0821 (7)	0.4110 (6)	0.5626 (5)	0.037 (4)
C8	0.1777 (6)	0.3420 (6)	0.5775 (5)	0.031 (4)
C11	−0.1992 (6)	0.1820 (5)	0.4049 (5)	0.031 (4)
C12	−0.2713 (7)	0.2306 (7)	0.3425 (5)	0.039 (5)
C13	−0.3701 (8)	0.1948 (7)	0.2916 (5)	0.043 (6)
C14	−0.3970 (8)	0.1091 (7)	0.3013 (6)	0.048 (7)
C15	−0.3258 (8)	0.0592 (6)	0.3626 (6)	0.048 (5)
C16	−0.2274 (7)	0.0957 (6)	0.4144 (6)	0.039 (5)
C21	−0.0369 (6)	0.1662 (5)	0.5636 (5)	0.027 (4)
C22	−0.1184 (7)	0.1661 (6)	0.6121 (5)	0.036 (4)
C23	−0.0987 (8)	0.1248 (6)	0.6871 (5)	0.047 (5)
C24	0.0026 (9)	0.0786 (6)	0.7174 (5)	0.048 (6)
C25	0.0839 (8)	0.0767 (6)	0.6712 (6)	0.050 (5)
C26	0.0642 (7)	0.1198 (6)	0.5946 (5)	0.041 (5)
C31	0.2733 (6)	0.4215 (5)	0.4544 (5)	0.035 (4)
C32	0.2512 (8)	0.4481 (6)	0.3715 (6)	0.045 (5)
C33	0.2937 (9)	0.5268 (7)	0.3510 (6)	0.057 (6)
C34	0.3552 (8)	0.5805 (6)	0.4129 (7)	0.054 (6)
C35	0.3766 (8)	0.5550 (6)	0.4955 (7)	0.050 (6)
C36	0.3363 (7)	0.4759 (6)	0.5162 (6)	0.043 (5)
C41	0.3556 (6)	0.2554 (5)	0.5182 (5)	0.029 (4)
C42	0.4273 (7)	0.2488 (6)	0.4637 (5)	0.041 (5)
C43	0.5257 (7)	0.1972 (7)	0.4843 (6)	0.050 (6)
C44	0.5523 (7)	0.1504 (7)	0.5577 (6)	0.044 (6)
C45	0.4821 (7)	0.1559 (7)	0.6119 (6)	0.044 (6)
C46	0.3845 (7)	0.2085 (6)	0.5920 (5)	0.039 (5)

[a] $U_{eq} = {}^1/_3 (U_{11} + U_{22} + U_{33})$.

(42) (a) Dickson, C.-A.; McFarlane, A. W.; Coville, N. J. *Inorg. Chim. Acta* **1989**, *158*, 205. (b) Hor, T. S. A.; Chan, H. S. O. *Ibid.* **1989**, *160*, 53.
(43) Sheldrick, G. M. SHELXS, University of Göttingen, Göttingen, Germany, 1986.
(44) *Structure Determination Package VAXSDP*; Enraf-Nonius: Delft, Netherlands.
(45) Walker, N.; Stuart, D. *Acta Crystallogr., Sect. A: Found. Crystallogr.* **1983**, *39A*, 158.

Acknowledgment. Support of this work by Deutsche Forschungsgemeinschaft, Bonn/Bad Godesberg, by Fonds der Chemischen Industrie, Frankfurt/Main, by BASF Aktiengesellschaft, and by Degussa AG is gratefully acknowledged. Thanks are also due to Prof. Dr. J. Strähle for providing the facilities for X-ray investigations and to Dr. A.-R. Grimmer for the measurements with the MSL 400 instrument and to W. P. Power for many helpful discussions.

Registry No. **1a**, 26743-81-7; **1b**, 15444-66-3; **1c**, 15553-68-1; **1d**, 15553-69-2; **1e**, 123110-09-8; **2a**, 41830-14-2; **2b**, 29890-05-9; **2c**, 50860-43-0; **2d**, 54111-75-0; **2e**, 122991-86-0; **3a**, 52595-94-5; **3b**, 14647-25-7; **3c**, 59329-00-9; **3d**, 65097-96-3; **3e**, 80537-31-1; **4**, 73573-46-3; K_2PtCl_4, 10025-99-7; $Mo(CO)_6$, 13939-06-5; $W(CO)_6$, 14040-11-0.

Supplementary Material Available: A figure of the molecular structure of **2d** with the complete labeling scheme and tables of final positional, isotropic, and anisotropic parameters and interatomic distances and angles for **2d** (14 pages); a listing of observed and calculated structure factors for **2d** (10 pages). Ordering information is given on any current masthead page.

Synthesis, Chemistry, and Structures of Mono-η^6-arene Complexes of Chromium(II) Bearing Trichlorosilyl and Carbon Monoxide Ligands

George N. Glavee, Balaji R. Jagirdar, Joerg J. Schneider,[1a] Kenneth J. Klabunde,*[1b] Lewis J. Radonovich,*[1c] and Kelly Dodd[1c]

Departments of Chemistry, Kansas State University, Manhattan, Kansas 66506, and University of North Dakota, Grand Forks, North Dakota 58202

Received August 30, 1991

(η^6-Arene)chromium tricarbonyl complexes have been photolyzed in the presence of trichlorosilane. The first reaction to take place is the expected loss of CO followed by oxidative addition to yield (η^6-arene)-$Cr(CO)_2(H)(SiCl_3)$. However, further photolysis causes the elimination of H_2 and formation of (η^6-arene)$Cr(CO)_2(SiCl_3)_2$. During this process the arene ligand becomes labilized and undergoes exchange with other arene ligands present. In some instances, the hydride intermediate is too short-lived to be isolated and the $-Cr(CO)_2(SiCl_3)_2$ derivative is preferentially formed. Evidence is presented that the presence of the $SiCl_3$ groups helps labilize the η^6-arene group both thermally and photochemically. Attempts to incorporate heteroatom-containing arenes are discussed, and X-ray structural elucidations of (η^6-mesitylene)$Cr(CO)_2(SiCl_3)_2$ and square-planar (2,4,6-collidine)$_2CrCl_2$ are presented.

Introduction

In 1971 Jetz and Graham reported on the oxidative addition of H–$SiCl_3$ to photochemically generated (benzene)$Cr(CO)_2$, yielding (benzene)$Cr(CO)_2(H)(SiCl_3)$.[2] Since that time extensive work on H–SiR_3 oxidative additions has been carried out by Schubert, Jaouen, Corriu, and their co-workers.[3] A variety of hydride–arene and Cp complexes of Mn, Cr, and Fe have been prepared, usually by photochemical decarbonylation followed by H–SiR_3 addition.

Initially our interest was in preparing similar derivatives and studying η^6-arene lability, as an extension of earlier work with somewhat analogous Co(II) and Ni(II) systems.[4,5] However, new results and new compounds were quickly discovered. It was found that two-step photolytic processes were possible, leading to (η^6-arene)$Cr(CO)_2$-$(SiCl_3)_2$ systems with enhanced η^6-arene labilities and other interesting properties.

Experimental Section

General Procedures. All reactions were carried out under Ar at room temperature using standard Schlenk[6] and inert atmosphere techniques unless otherwise stated. Tetrahydrofuran (THF) and diethyl ether (Et_2O) were distilled under Ar from

(1) (a) On leave from the Max-Planck-Institute für Kohlenforschung, 4330 Mulheim/Ruhr, Germany. (b) Kansas State University. (c) University of North Dakota.

(2) Jetz, W.; Graham, W. A. G. *Inorg. Chem.* **1971**, *10*, 4.

(3) (a) Schubert, U.; Müller, J.; Alt, H. G. *Organometallics* **1987**, *6*, 469. (b) Matarasso-Tchoroulechine, E.; Jaouen, G. *Can. J. Chem.* **1988**, *66*, 2157. (c) Schubert, U. *Adv. Organomet. Chem.* **1990**, *30*, 151 and references therein. (d) Schubert, U.; Ackerman, K.; Kraft, G.; Wörle, B. *Z. Naturforsch.* **1983**, *38b*, 1488. (e) Colomer, E.; Corriu, R. J. P.; Vioux, A. *Inorg. Chem.* **1979**, *18*, 695. (f) Colomer, E.; Corriu, R. J. P.; Marzin, C.; Vioux, A. *Inorg. Chem.* **1982**, *21*, 368. (g) Carré, F.; Colomer, E.; Corriu, R. J. P.; Vioux, A. *Organometallics* **1984**, *3*, 971. (h) Matarasso-Tchiroukhine, E.; Jaouen, G. *Can. J. Chem.* **1988**, *66*, 2157. (i) Knorr, M.; Schubert, U. *Transition Met. Chem.* **1986**, *11*, 269. (j) Schubert, U. *Transition Met. Chem.* **1991**, *16*, 136.

(4) (a) Anderson, B. B.; Behrens, C. L.; Radonovich, L. J.; Klabunde, K. J. *J. Am. Chem. Soc.* **1976**, *98*, 5390. (b) Gastinger, R. G.; Anderson, B. B.; Klabunde, K. J. *J. Am. Chem. Soc.* **1980**, *102*, 4959. (c) Groshens, T. J.; Klabunde, K. J. *Organometallics* **1982**, *1*, 564. (d) Lin, S. T.; Narske, R. N.; Klabunde, K. J. *Organometallics* **1985**, *3*, 571. (e) Brezinski, M. M.; Klabunde, K. J. *Organometallics* **1983**, *2*, 1116. (f) Groshens, T. J.; Klabunde, K. J. *J. Organomet. Chem.* **1983**, *259*, 337. (g) Klabunde, K. J.; Anderson, B. B.; Neuenschwander, K. *Inorg. Chem.* **1980**, *19*, 3719.

(5) (a) Choe, S. B.; Kanai, H.; Klabunde, K. J. *J. Am. Chem. Soc.* **1989**, *111*, 2875. (b) Choe, S. B.; Schneider, J. J.; Klabunde, K. J.; Radonovich, L. J.; Ballantine, T. A. *J. Organomet. Chem.* **1989**, *376*, 419. (c) Brezinski, M. M.; Schneider, J. J.; Radonovich, L. J.; Klabunde, K. J. *Inorg. Chem.* **1989**, *28*, 2414.

(6) (a) Shriver, D. F.; Drezdon, M. A. *The Manipulation of Air Sensitive Compounds*, 2nd ed.; Wiley, New York, 1986. (b) Herzog, S.; Dehnert, J.; Luhder, K. In *Technique of Inorganic Chemistry*; Johnassen, H. B., Ed.; Interscience: New York, 1969; Vol. VII.

0276-7333/92/2311-1043$03.00/0